Soft Matter

PAPER

Force and stroke of a hydrogel actuator

Widusha R. K. Illeperuma,[ab] Jeong-Yun Sun,[ab] Zhigang Suo[ab] and Joost J. Vlassak*[a]

Hydrogels that undergo a volume phase transition in response to an external stimulus are of great interest because of their possible use as actuator materials. The performance of an actuator material is normally characterized by its force–stroke curve, but little is known about the force–stroke behavior of hydrogels. We use the theory of the ideal elastomeric gel to predict the force–stroke curves of a temperature-sensitive hydrogel and introduce an experimental method for measuring the curve. The technique is applied to PNIPAm hydrogels with low cross-link densities. The maximum force generated by the hydrogel increases with increasing cross-link density, while the maximum stroke decreases. The force–stroke curves predicted by the theory of the ideal elastomeric gel are in very good agreement with the experimental curves.

Introduction

A hydrogel consists of a network of cross-linked hydrophilic polymer chains dispersed in water. The water concentration in the gel, and hence its degree of swelling, can vary markedly with the temperature,[1–3] pH[4,5] or even electric field.[6] This ability to respond to an external stimulus can be used in a range of applications, including sensors,[7,8] actuators in microfluidic devices[9–11] and drug delivery.[12,13] Here we are interested in exploring the performance of hydrogels in actuator applications. Actuators are usually characterized by their force–stroke curves.[14,15] The stroke of an actuator is defined as the displacement achieved by the actuator under a given force, critical information when designing an actuator. In general, stroke and force are inversely related.[14,16,17] Even though the concept of a force–stroke curve is widely used in the field of actuators, it is not used in the field of hydrogels. Free swelling of hydrogels has of course been studied extensively, but constrained swelling where the hydrogel exerts a force is much less explored;[3,18] complete force–stroke curves for hydrogels are not currently available in the literature.

We derive expressions for the force–stroke curve of a hydrogel and explore the use of force–stroke curves to characterize the actuating properties of hydrogels, using poly(*N*-isopropylacrylamide) as a model material. Poly(*N*-isopropylacrylamide), commonly abbreviated as PNIPAm, is a widely studied temperature-sensitive hydrogel. PNIPAm hydrogels exhibit a reversible, continuous volume phase transition, when the temperature is increased above the critical temperature T_c.[1,19] The volume phase transition is attributed to a coil–globule

transition of the polymer chains that occurs at this temperature.[20] As illustrated in Fig. 1, the hydrogel can absorb a large amount of water at temperatures below T_c, but not at higher temperatures. This ability to swell and shrink in response to a temperature change makes PNIPAm a candidate for use in actuators.

In this paper, we first use the model of the ideal elastomeric gel[21,22] to predict the force–stroke curves of a temperature-sensitive hydrogel. We then describe an experimental method for measuring the force–stroke curves and evaluate the effect of cross-link density. We demonstrate very good agreement between the theoretical curves and the experimental measurements for a broad range of cross-link densities.
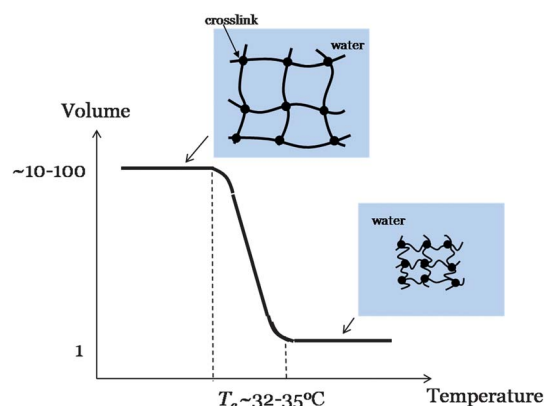

Fig. 1 Volume phase transition of PNIPAm hydrogels. In the figure, the *y*-axis is the volume of the hydrogel relative to the volume of the dry polymer network. A swollen PNIPAm hydrogel is ∼10–100 times the volume of the dry polymer network. Upon heating the PNIPAm hydrogel, the volume drastically reduces in the range of T_c ∼ 32–35 °C. At high temperature, the volume of the hydrogel approaches the volume of the dry polymer network.

[a]*School of Engineering and Applied Sciences, Harvard University, Cambridge, MA 02138, USA. E-mail: vlassak@seas.harvard.edu*
[b]*Kavli Institute for Bionano Science and Technology, Harvard University, Cambridge, MA, 02138, USA*

The ideal elastomeric hydrogel

According to the classical theory of Flory and Rehner,[23] the elasticity of a polymer network can be described by the Gaussian chain model, while the mixing of polymer and solvent can be described by the Flory–Huggins model.[24,25] These original models have often been modified to fit experimental data.[2,26] Here we use the model of the ideal elastomeric gel,[21] which does not invoke the Flory–Huggins model, but instead relies on the following two basic assumptions. First, the volume of the gel is equal to the sum of the volume of the dry polymer network and the absorbed solvent. Second, the Helmholtz free energy of the gel is separable into a contribution due to stretching of the network and one due to mixing of polymer and solvent. The latter is conveniently represented by the osmotic pressure as a function of the swelling ratio, $\Pi_{mix}(J)$. Li *et al.*[22] verified the model of the ideal elastomeric gel for polyacrylamide gels and demonstrated that the $\Pi_{mix}(J)$ obtained through different experimental methods is consistent.

We use the model of the ideal elastomeric gel to describe the chemo-mechanical behavior of a temperature-sensitive hydrogel. Consider a stress-free cube of dry gel with unit dimensions as shown in Fig. 2. We take this state as the reference state. In the current state, the gel is submerged in an aqueous environment in which the chemical potential of water is μ, and the gel is subjected to Cauchy stresses σ_1, σ_2, and σ_3. By convention, the chemical potential of pure liquid water is set to zero. The gel absorbs C water molecules and turns into a block of dimensions $\lambda_1 \times \lambda_2 \times \lambda_3$. The swelling ratio J is then given by $J = \lambda_1\lambda_2\lambda_3$. If we take the Gaussian chain model to describe the mechanical behavior of the polymer network, the equations of state of a swelling hydrogel can be written as,[21,22,27]

$$\sigma_1 = \frac{NkT}{J}\left(\lambda_1{}^2 - 1\right) - \Pi_{mix}(J, T) - \frac{\mu}{\Omega}, \tag{1a}$$

$$\sigma_2 = \frac{NkT}{J}\left(\lambda_2{}^2 - 1\right) - \Pi_{mix}(J, T) - \frac{\mu}{\Omega}, \tag{1b}$$

$$\sigma_3 = \frac{NkT}{J}\left(\lambda_3{}^2 - 1\right) - \Pi_{mix}(J, T) - \frac{\mu}{\Omega} \tag{1c}$$

$$J = 1 + \Omega C \tag{1d}$$

where N is the crosslink density of the gel, kT is the temperature in units of energy, and Ω is the volume per water molecule. The osmotic pressure has two contributions: $\Pi_{mix}(J, T)$ is the osmotic pressure inside the hydrogel in equilibrium with pure water, and μ/Ω is the additional contribution when the hydrogel is in equilibrium with an aqueous environment in which the chemical potential of water is different from zero. Π_{mix} is a function of the swelling ratio J and the temperature T, but not of the crosslink density of the gel.[22] The quantity NkT is the shear modulus of the dry polymer network. The Gaussian chain model is not an essential part of the ideal elastomeric gel model. Any model that accurately describes the mechanical behavior of the polymer network can be used.

According to eqn (1), the applied stresses are balanced by the stresses that arise because of the elastic deformation of the polymer network and the total osmotic pressure inside the gel. To fully characterize the response of a temperature-sensitive gel that follows the Gaussian chain model, it is sufficient to know the scalar NkT and the function $\Pi_{mix}(J, T)$. If we fix the temperature, then $\Pi_{mix}(J)$ is a single variable function that does not depend on the crosslink density and that is a unique function for each type of hydrogel.

Derivation of the force–stroke curves

Consider a hydrogel immersed in pure liquid water ($\mu = 0$). When subjected to a change in temperature, the hydrogel goes through a volume phase transition. As the volume changes, the hydrogel is free to expand or contract in the x_1 and x_2-directions, but exerts a force in the x_3-direction. Fig. 3 illustrates schematically how to generate the force–stroke curve for the hydrogel. The reference state of the hydrogel is a cube of the hydrogel in the dry state, at a temperature above the critical temperature, T_c. The length of the cube edge is designated by H. If the gel is allowed to swell under zero external force at a temperature below T_c, it forms a cube with the edge length h. The corresponding actuator displacement, $h–H$, is defined as the "free stroke". If the height of the gel is limited to $h_3 < h$, then swelling is constrained and the gel generates a force F. The force
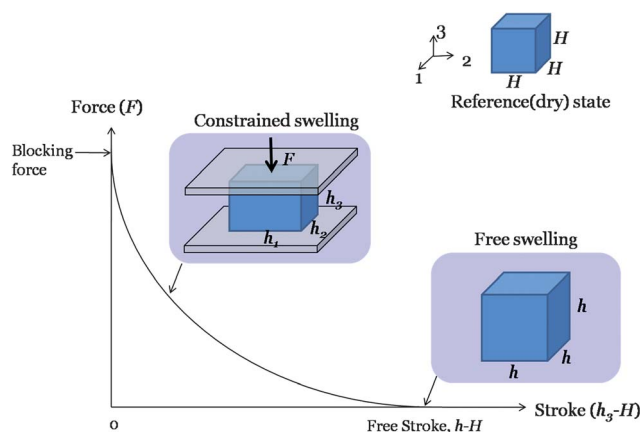
Fig. 3 Force–stroke curve of a hydrogel actuator. In the reference state, the gel is dry and forms a cube with side H. F is the actuation force and $h_3–H$ is the stroke. When the hydrogel swells freely without applying any force, it generates the maximum stroke, $h–H$, called the free stroke. If the hydrogel swells under constraint, it generates a force that increases with decreasing stroke. The hydrogel generates the maximum, or blocking, force at zero stroke.
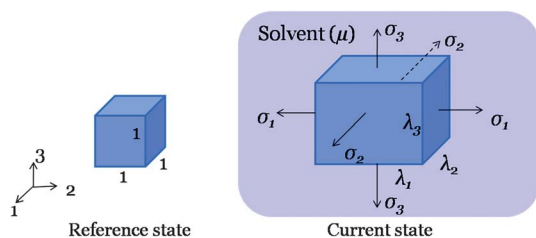

Fig. 2 The reference state is a dry polymer network of unit dimensions, subjected to no applied stresses. The current state is a swollen gel stretched into a rectangular block. The gel is submerged in an aqueous environment in which the chemical potential of water is μ, and is subjected to stresses σ_1, σ_2, and σ_3.

that completely blocks swelling in the x_3-direction, *i.e.*, $h_3 = H$, is referred to as the blocking force. The stretches are defined by $\lambda_1 = h_1/H$, $\lambda_2 = h_2/H$, and $\lambda_3 = h_3/H$, the true stress is defined by $\sigma_3 = F/(h_1 h_2)$, and the nominal stress is defined by $s_3 = F/H^2$.

We derive the force–stroke curves based on the model of the ideal elastomeric gel. In the current state, $\sigma_1 = \sigma_2 = 0$ and $\lambda_1 = \lambda_2$. Thus the swelling ratio can be written as $J = \lambda_1^2 \lambda_3$. From eqn (1a), it follows that

$$\frac{NkT}{\lambda_1^2 \lambda_3}(\lambda_1^2 - 1) - \Pi_{\mathrm{mix}}(J, T) = 0, \tag{2}$$

where μ/Ω was set to zero because the hydrogel is in equilibrium with pure water. If the function $\Pi_{\mathrm{mix}}(J)$ is known for the hydrogel, eqn (2) can be used to calculate λ_1 as a function of λ_3. Eqn (1c) then yields

$$\sigma_3 = NkT\left(\lambda_3 - \frac{1}{\lambda_3}\right) - \Pi_{\mathrm{mix}}(J, T)\lambda_3^2 \tag{3}$$

And the nominal stress becomes,

$$s_3 = NkT\lambda_1^2\left(\lambda_3 - \frac{1}{\lambda_3}\right) - \Pi_{\mathrm{mix}}(J, T)\lambda_1^2 \lambda_3^2. \tag{4}$$

This is the expression for the force–stroke curve of a hydrogel. The derived force–stroke relationship is the steady-state relationship; solvent migration makes the actual performance of a gel actuator highly time-dependent. It is evident from eqn (4) that the force–stroke curve can be calculated if the function $\Pi_{\mathrm{mix}}(J, T)$ is known. Fig. 4 shows this relationship for PNIPAm hydrogels using the $\Pi_{\mathrm{mix}}(J, T)$ curve measured using the procedure described in the next section. It is observed that the blocking force ($\lambda_3 = 1$) increases with increasing cross-link density, while the free stroke ($s_3 = 0$) decreases.

A procedure for measuring $\Pi_{\mathrm{mix}}(J)$

The force–stroke curve of a hydrogel requires knowledge of the $\Pi_{\mathrm{mix}}(J, T)$ function. Here we describe a simple procedure for measuring this function experimentally based on free swelling of gels in environments with controlled chemical potentials. Under conditions of free swelling, no stresses are applied to the

gel and swelling is isotropic. If $\lambda_1 = \lambda_2 = \lambda_3 = \lambda_f$, then eqn (1) implies that

$$\sigma_1 = \frac{NkT}{\lambda_f^3}(\lambda_f^3 - 1) - \Pi_{\mathrm{mix}}(J, T) - \frac{\mu}{\Omega} = 0. \tag{5}$$

Solving for the osmotic pressure yields

$$\Pi_{\mathrm{mix}}(J, T) = G\left(1 - \frac{1}{\lambda_f^2}\right) - \frac{\mu}{\Omega}, \tag{6}$$

where $G = NkT/\lambda_f$ is the shear modulus of the gel in the swollen state. It is clear from eqn (6) that the osmotic pressure can be determined by measuring the free-swelling stretches as a function of the chemical potential of water in the environment. These measurements can be implemented using the following approach suggested in ref. 28 and 29. Enclose a hydrogel in a flexible water-permeable membrane and submerge it in a mixture of water and a second compound. This second compound needs to satisfy two conditions: (1) the compound cannot migrate through the membrane and (2) the chemical potential of water in the mixture must be well known, *e.g.*, through a series of osmotic pressure experiments such as those described in ref. 30 and 31. If the chemical potential of water in the hydrogel is different from that in the mixture, water will migrate through the membrane to equalize the potentials and the gel will expand or shrink, as may be the case. The flexible membrane serves to prevent the second compound from diffusing into the gel and thus change the chemical environment, but it does not impede the volume change in any way. Once the equilibrium is established, the function $\Pi_{\mathrm{mix}}(J, T) = \Pi_{\mathrm{mix}}(\lambda_f^3, T)$ can be calculated from the chemical potential of water in the mixture and the stretch λ_f using eqn (6). Repetition of this procedure for different water mixtures and temperatures establishes $\Pi_{\mathrm{mix}}(J, T)$ as a function of J and T.

Experimental

Sample fabrication

PNIPAm hydrogels were prepared using the following procedure: 1.1111 g of *N*-isopropylacrylamide (NIPA, Sigma-Aldrich, 415324) and different amounts of *N*-*N*-methylenebisacrylamide (MBAA, Sigma-Aldrich, M7279) were dissolved in distilled water as shown in Table 1. To these mixtures, 9.889 mg of ammonium persulfate (AP, Sigma-Aldrich, A9164) was added as a photo-initiator and 25.56 mg of *N*,*N*,*N'*,*N'*-tetramethylethylenediamine (TEMED, Sigma-Aldrich, T1024) was added as a cross-link accelerator. The solutions were poured into glass molds with dimensions $70 \times 30 \times 3$ mm^3 and covered with glass slides. The gels were cured at room temperature by exposing them to ultraviolet light with a wavelength of 254 nm and a power of 8 W for a period of 4 hours inside a UVC 500 system (Hoefer). This procedure resulted in PNIPAm hydrogels with various levels of cross-linking as listed in Table 1.
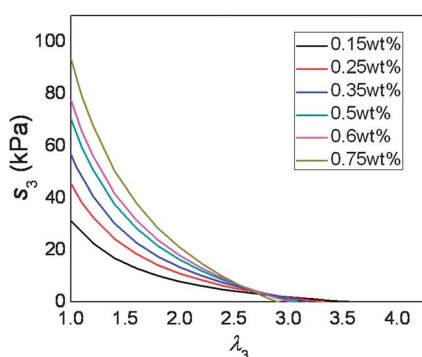

Fig. 4 Force–stroke curves for PNIPAm hydrogels with different cross-link densities, derived using the ideal elastomeric gel theory and the experimentally measured $\Pi_{\mathrm{mix}}(J, T)$ function. The force is converted to nominal stress s_3 and the stroke is converted to stretch λ_3. The blocking force ($\lambda_3 = 1$) increases and the free stroke ($s_3 = 0$) decreases with increasing cross-link density.

Characterization of $\Pi_{\mathrm{mix}}(J, T)$

The $\Pi_{\mathrm{mix}}(J, T)$ function was measured for the PNIPAm samples using the procedure outlined earlier in this paper. Immediately

Table 1 Synthesis data for PNIPAm hydrogels

Sample	Amount of MBAA (mg)	$\dfrac{W_{MBAA}}{W_{MBAA} + W_{NIPAm}} \times 100\%$
1	1.7	0.15
2	2.8	0.25
3	3.9	0.35
4	5.6	0.5
5	6.7	0.6
6	8.4	0.75

after synthesis, PNIPAm samples with different cross-link densities were submerged in mixtures of water and polyethylene glycol (PEG, BioUltra, MW 20 000, Sigma-Aldrich 95172), which is a convenient method of controlling the chemical potential of water in the environment. PEG was selected because it is a water-soluble polymer that is readily available in different molecular weights. Mixtures of PEG and water have been extensively characterized and the chemical potential of water in these mixtures is well known (Fig. 5(a)).[30,31] To prevent the PEG from diffusing into the PNIPAm, the samples were enclosed inside dialysis bags (cellulose membrane, Sigma Aldrich D9527) along with a small amount of deionized water (Fig. 5(b)). Dialysis bags were selected as water-permeable membranes because the pores in dialysis membranes allow water to pass through, but not PEG. The dialysis bags were much larger than the samples, so that they did not exert any mechanical constraint on the samples. This experiment was performed right after synthesizing the PNIPAm samples so that their water content was fixed at approximately 90% for all samples. Six different water–PEG solutions were prepared with PEG concentrations of 0, 0.025, 0.05, 0.505 and 1.282 mmol l^{-1}. All experiments were performed at 20 °C. The samples, $10 \times 10 \times 3$ mm^3 in size, were submerged for a period of one week, which was sufficient to establish equilibrium between the sample and the PEG solution. The samples were then removed from the dialysis bags, any surface water present was removed by blotting with a tissue paper, and the free swelling ratio, λ_f, was measured for each sample using the gravimetric method. Specifically, the samples were weighed using an analytical scale to obtain the weight, W_{gel}, of the samples in equilibrium with the PEG solution. The

weight of the dry samples, W_{dry}, was determined after freeze-drying the samples. This was accomplished by freezing the samples at -80 °C and then transferring them to a freeze-dry system (Labconco Corporation) at a temperature of -50 °C. The samples were removed from the freeze-dry system after 3 days when they were fully dehydrated. The free swelling ratio, λ_f, was calculated from

$$\lambda_f = \left(\frac{W_{gel}}{W_{dry}}\right)^{1/3}. \tag{7}$$

The osmotic pressure was calculated from λ_f and μ using eqn (6). Because all measurements were performed at 20 °C, we denote $\Pi_{mix}(J, T)$ henceforth as $\Pi_{mix}(J)$.

Mechanical characterization and measurement of force–stroke curves

Uniaxial compression tests were performed using an AR-G2 rheometer (TA instruments) as shown in Fig. 6(a). Rectangular samples with dimensions of $4 \times 4 \times 3$ mm^3 were compressed at a rate of 100 μm min^{-1} until a strain of 5% was reached. Young's modulus was calculated from the slope of the stress–strain curves and the shear modulus, G, was obtained as one third of the Young's modulus on the assumption that hydrogels are incompressible at small strains and on the time scale of the experiment. A total of three PNIPAm samples were tested for each cross-link density.

The force–stoke curves were measured following the approach described earlier. Specifically, after synthesis the PNIPAm gels were allowed to fully swell in DI water at room temperature. Cylindrical samples with a diameter of 10 mm were cut from the swollen gels using a hole punch. The thickness of the samples was approximately 5 mm, but varied somewhat with the cross-link density. These samples were heated to 50 °C and kept at this temperature for three days to allow them to reach their dry equilibrium state. The dried samples were then allowed to cool to room temperature before performing constrained swelling experiments inside the AR-G2 rheometer. The initial state is shown schematically in Fig. 6(b), where a dry PNIPAm sample is placed between two rigid plates and submerged in water at 20 °C. The sample swells by absorbing water and generates a force when it touches the
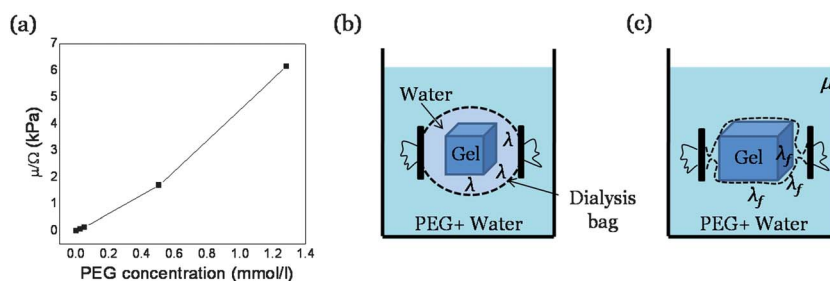

Fig. 5 Free swelling of hydrogels in equilibrium with an aqueous solution of PEG. (a) Chemical potential of water in aqueous solutions of PEG.[30,31] (b) Freshly prepared PNIPAm hydrogels are enclosed inside dialysis bags containing deionized water and are immersed in various concentrations of water–PEG solutions. The stretch λ represents the stretch of the freshly prepared sample with respect to its dry reference state. (c) When the hydrogel equilibrates with the water–PEG solution, all water in the dialysis bag disappears. The free stretch λ_f represents the stretch of the equilibrated sample with respect to its dry reference state.
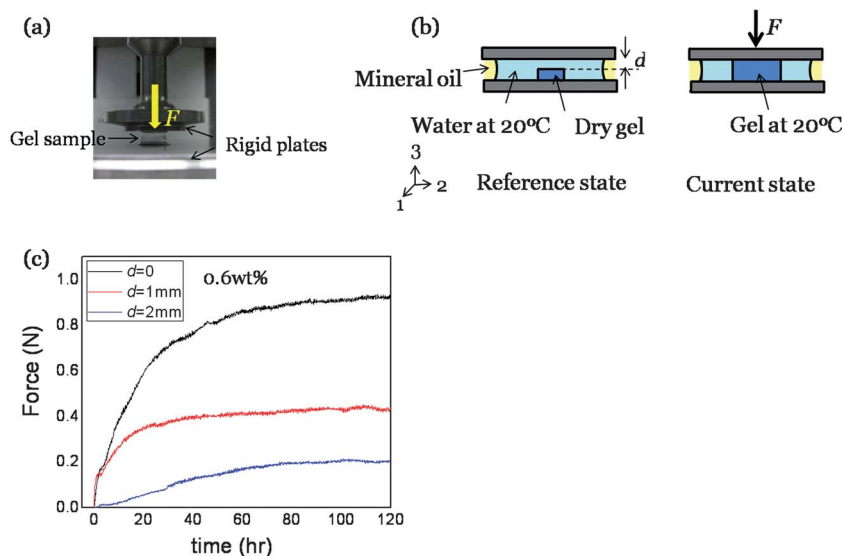
Fig. 6 Mechanical characterization and measurement of the force–stroke curves. (a) Uniaxial compression test for measuring the shear modulus. Hydrogels were compressed under two rigid plates and the force–displacement data were recorded to obtain the shear modulus. (b) Setup for the constrained swelling experiment. The reference state shows a dry PNIPAm gel submerged in water at 20 °C; this gel is placed between two rigid plates with a gap, d, between the sample and the upper plate. Mineral oil is used to prevent water evaporation during the experiment. The current state shows the swollen gel in the equilibrium state. The force F generated by the hydrogel is recorded as a function of time until it saturates. (c) Force–time curve for a 0.6 wt% PNIPAm hydrogel and for different values of d.

upper plate. This force was recorded as a function of time until the sample was fully saturated and the force reached a steady-state value as shown in Fig. 6(c). Force–time curves were measured as a function of the initial gap d between the sample and the plate (Fig. 6(b)). The saturation force was converted to a nominal stress by normalizing the force with the initial cross-sectional area of the sample; the stroke was converted to stretch, λ, by normalizing with the initial sample height. Force stroke curves were measured for all PNIPAm samples listed in Table 1. The subscript 3 in the remainder of the text refers to the loading direction.

Results and discussion

Fig. 7(a) shows the free swelling ratio, λ_f, as a function of PEG concentration for PNIPAm samples with different levels of cross-linking; Fig. 7(b) shows the corresponding shear moduli. Together with the chemical potential of water in aqueous PEG solutions, Fig. 5(a), these experimental results can be used to calculate $\Pi_{\mathrm{mix}}(J)$ from eqn (6). The result is plotted in Fig. 7(c). Even though samples with different cross-link densities have different shear moduli and different swelling ratios, their osmotic pressure functions collapse into a single master curve. This master curve is independent of the cross-link density and can be regarded as a material property of PNIPAm hydrogels. Evidently, the cross-link density of the hydrogels is low enough that the cross-links do not substantially alter the chemical interactions between the PNIPAm polymer chains and the surrounding water. This observation is not unique to PNIPAm, but has also been established for other gels such as poly-acrylamide gels.[22] Even though the osmotic function was derived from free-swelling data, it can be used to predict the

behavior of PNIPAm hydrogels under complex conditions of loading and in various chemical environments. It is convenient to represent the data in Fig. 7(c) by a curve fit

$$\Pi_{\mathrm{mix}}(J) = 0.2 + 50 \times \exp(-0.138J) \text{ kPa}, \qquad (8)$$

which is valid at 20 °C in the range $12 < J < 65$.

Fig. 8 shows normalized force–stroke or stress–stretch curves for samples with different cross-link densities. Black squares correspond to experimental data and the red lines are predictions based on the ideal elastomeric model, eqn (4), and the curve fit to the osmotic pressure function, eqn (8). The shape of the curves in Fig. 8 is typical for force–stroke curves: the force is greatest when the actuator is blocked and decreases with increasing stroke. The blocking force increases with increasing crosslink density, while the free stroke decreases. The effect of cross-link density on the free swelling of PNIPAm hydrogels is well documented in the literature;[32,33] an increase in the cross-link density decreases the free swelling without changing the transition temperature. This observation is consistent with our results that the free stroke decreases with cross-link density. The effect on the blocking force is, however, subtler; as the cross-link density increases, the hydrogel becomes stiffer and swells less. The blocking force depends on both of these factors. Even though our experimental results show that the blocking force increases with increasing cross-link density, it is clear that the gel cannot generate a large blocking force when the cross-link density is too high. This can be understood as follows. In the limit of no cross-links at all, the stiffness of the hydrogel vanishes and the blocking force approaches zero. If, on the other hand, the cross-link density is very high, the stiffness of the hydrogel is very large and the free-swelling ratio approaches one. The hydrogel cannot swell and generates no blocking force.
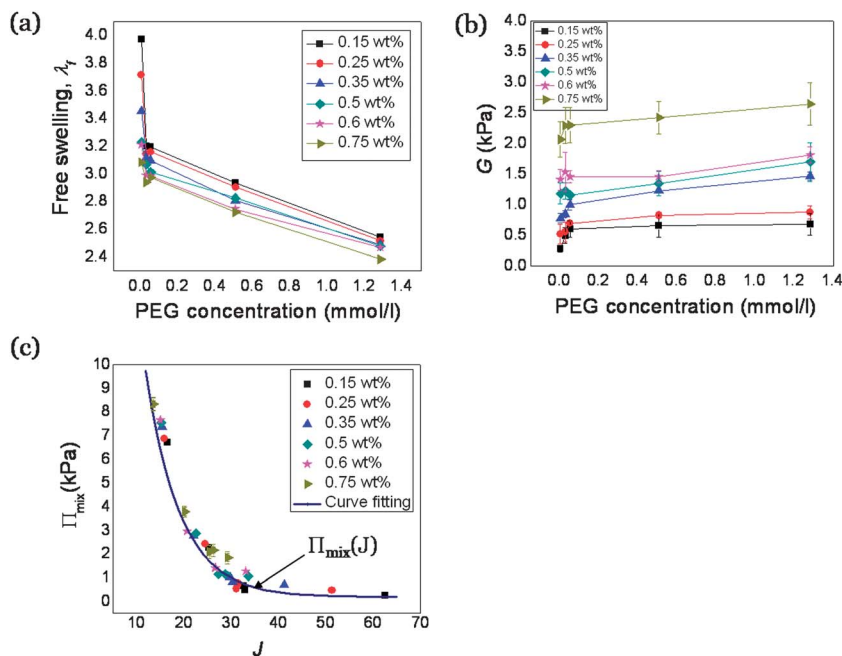
Fig. 7 Determination of the osmotic pressure function $\Pi_{mix}(J)$. (a) Free swelling ratio λ_f of PNIPAm hydrogels as a function of PEG concentration. Curves with different symbols represent the free swelling ratios for hydrogels with different cross-link densities. (b) Shear modulus of PNIPAm hydrogels with different cross-link densities as a function of PEG concentration. (c) Experimental values of the osmotic pressure for PNIPAm hydrogels with different cross-link densities. Data for different cross-link densities collapse into a single $\Pi_{mix}(J)$ curve.

Consequently the blocking force must peak at an intermediate level of cross-linking. This prediction is illustrated in Fig. 9, where the blocking stress derived from eqn (6) is plotted as a function of NkT. Phase separation[34] in the PNIPAm hydrogels prevented us from confirming this behavior at large cross-link densities, but it may be possible to access this regime in other hydrogels.

In many applications, a quick and uniform actuator response is required. The speed with which a hydrogel actuator responds to a stimulus is governed by the diffusion of water into or out of the hydrogel and depends sensitively on the size of the actuator. The response time of a micrometer-sized gel particle, for instance, is on the order of 10^{-2} to 10^{-4} s, making it a viable actuator for a range of micro-fluidic applications. Even though
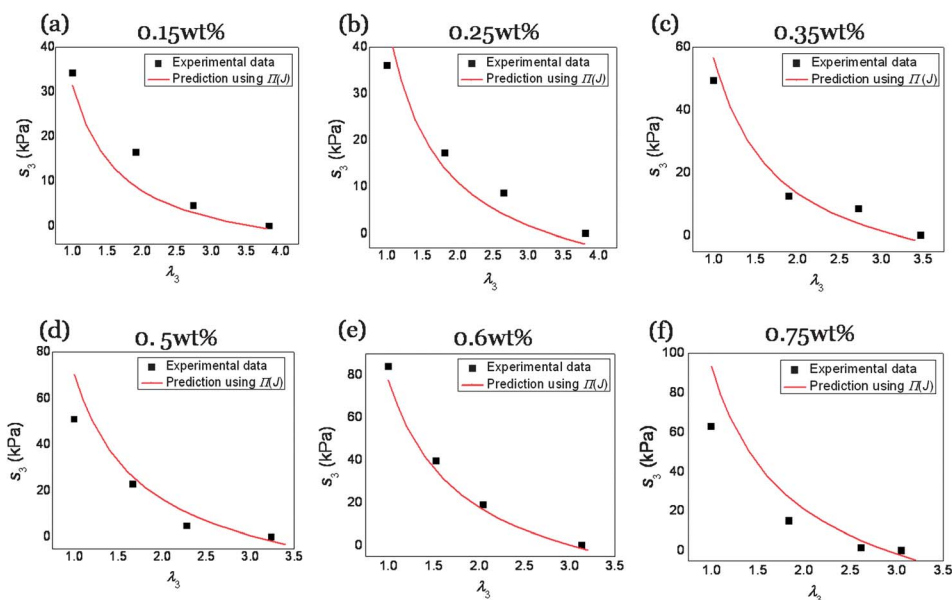

Fig. 8 Force–stroke curves. The force is converted to nominal stress s_3 and the stroke is converted to stretch λ_3. Curves (a)–(f) show s_3–λ_3 curves for PNIPAm hydrogels with different cross-link densities. Cross-link weight percentages are denoted for each curve. Black squares correspond to experimental results and curves are predictions from the ideal elastomeric model.
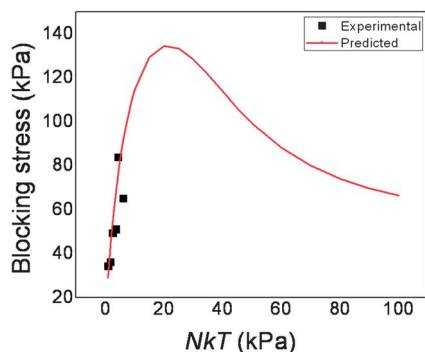
Fig. 9 Blocking force as a function of cross-link density. The solid curve is a prediction based on the $\Pi_{mix}(J, T)$ relationship.

the experiments presented in this paper were performed on millimeter-size samples, the results and analysis are directly applicable to gels on the micrometer scale.

Conclusion

We have used the ideal elastomeric gel model to derive the force–stroke curves of hydrogel actuators. The force–stroke curves depend on the shear modulus and on the osmotic pressure function of the hydrogel. We have described simple methods for measuring the osmotic pressure function and the force–stroke curves. Measurement of the osmotic pressure curves for PNIPAm samples with different cross-link densities shows that the osmotic pressure function is independent of the cross-link density. The experimental force–stroke curves are in very good agreement with the model predictions, demonstrating that the ideal elastomeric gel model provides a very general description of the behavior of a hydrogel for a broad range of loading conditions, chemical environments, and cross-link densities.

Acknowledgements

References

1 Y. Hirokawa and T. Tanaka, Volume phase transition in a non ionic gel, *J. Chem. Phys.*, 1984, **81**(12), 6379–6380.

2 H. Shirota, N. Endo and K. Horie, Volume phase transition of polymer gel in water and heavy water, *Chem. Phys.*, 1998, **238**, 487–494.

3 S. Cai and Z. Suo, Mechanics and chemical thermodynamics of phase transition in temperature –sensitive hydrogels, *J.Mech.Phys.Solids*, 2011, **59**, 2259–2278.

4 L. B. Peppas and N. A. Peppas, Equilibrium swelling behavior of pH-sensitive hydrogels, *Chem. Eng. Sci.*, 1991, **46**, 715–722.

5 L. Zarzar, P. Kim and J. Aizenberg, Bio-inspired design of submerged hydrogel-actuated polymer microstructures operating in response to pH, *Adv. Mater.*, 2011, **23**, 1442–1446.

6 T. Tanaka, I. Nishio, S. T. Sun and S. U. Nishio, Collapse of gels in an electric field, *Science*, 1982, **218**, 467–469.

7 M. Guenther, D. Kuckling, C. Corten, G. Gerlach, J. Sorber, G. Suchaneck and K.-F. Arndt, Chemical sensors based on multiresponsive block copolymer hydrogels, *Sens. Actuators, B*, 2007, **126**, 97–106.

8 R. Bashir, J. Z. Hilt, O. Elibol, A. Gupta and N. A. Peppas, Micromechanical cantilever as an ultrasensitive pH microsensor, *Appl. Phys. Lett.*, 2002, **81**, 3091–3093.

9 M. E. Harmon, M. Tang and C. W. Frank, A microfluidic actuator based on thermoresponsive hydrogels, *Polymer*, 2003, **44**, 4547–4556.

10 D. J. Beebe, J. S. Moore, J. M. Bauer, Q. Yu, R. H. Liu, C. Devadoss and B.-H. Jo, Functional hydrogel structures for autonomous flow control inside microfluidic channels, *Nature*, 2000, **404**, 588–590.

11 A. Richter, S. Howitz, D. Kuckling and K.-F. Arndt, Influence of volume phase transition phenomena on the behavior of hydrogel- based valves, *Sens. Actuators, B*, 2004, **99**, 451–458.

12 R. Langer, Drug delivery and targeting, *Nature*, 1998, **392**, 5–10.

13 R. Dinarvand and A. D'Emanuele, The use of thermoresponsive hydrogels for on-off release of molecules, *J. Controlled Release*, 1995, **36**, 221–227.

14 G. M. Spinks, L. Liu, G. G. Wallace and D. Zhou, Strain response from Polypyrrole actuators under load, *Adv. Funct. Mater.*, 2002, **12**, 437–440.

15 R. Kornbluh, R. Pelrine, J. Eckerle and J. Joseph, Electrostrictive polymer artificial muscle actuators, in *Proc. IEEE Intl. Conf. Rob. Autom.Leuven*, Belgium, 1998, pp. 2147–2154.

16 F. F. C. Duval, S. A. Wilson, G. Ensell, N. M. P. Evanno, M. G. Cain and R. W. Whatmore, Characterization of PZT thin film micro-actuators using a silicone micro-force sensor, *Sens. Actuators, A*, 2006, **133**, 35–44.

17 R. Shankar, T. K. Ghosh and R. J. Spontak, Dielectric elastomers as next generators polymeric actuators, *Soft Matter*, 2007, **3**, 1116–1129.

18 A. Suzuki and S. Kojima, Phase transition in constrained polymer gels, *J. Chem. Phys.*, 1994, **11**, 10003–10007.

19 H. G. Schild, Poly(*N*-isopropylacrylamide): experiment, theory and applications, *Prog. Polym. Sci.*, 1992, **17**, 163–249.

20 C. Wu and X. Wang, Globule-to-coil transition of a single homopolymer chain in solution, *Phys. Rev. Lett.*, 1998, **80**, 4092–4094.

21 S. Cai and Z. Suo, *Equations of state for ideal elastomeric gels*, EPL, 2012, vol. 34009, pp. 1–6.

22 J. Li, Y. Hu, J. J. Vlassak and Z. Suo, Experimental determination of equations of state for ideal elastomeric gels, *Soft Matter*, 2012, **8**, 8121–8128.

23 P. J. Flory and J. Rehner, Statistical mechanics of cross-linked polymer networks II. Swelling, *J. Chem. Phys.*, 1943, **11**(11), 521–526.

24 P. J. Flory, Thermodynamics of high polymer solutions, *J. Chem. Phys.*, 1942, **10**(1), 51–61.

25 M. L. Huggins, Solutions of long chain compounds, *J. Chem. Phys.*, 1941, **9**(5), 440.

26 S. Hirotsu, Y. Hirokawa and T. Tanaka, Volume-phase transitions of ionized N isopropylacrylamide gels, *J. Chem. Phys.*, 1987, **87**(2), 1392–1395.

27 W. Hong, X. Zhao, J. Zhou and Z. Suo, A theory of coupled diffusion and large deformation in polymeric gels, *J. Mech. Phys. Solids*, 2008, **56**, 1779–1793.

28 F. Horkay, I. Tasaki and P. Basser, Effect of monovalent-divalent cation exchange on the swelling of polyacrylate hydrogels in physiological salt solutions, *Biomacromolecules*, 2001, **2**, 195–199.

29 B. G. Stubbe, *et al.*, Tailoring the swelling pressure of degrading Dextran Hydroxyethyl Methacrylate hydrogels, *Biomacromolecules*, 2003, **4**, 691–695.

30 V. A. Parsegian, R. P. Rand, N. L. Fuller and D. C. Rau, Osmotic stress for the direct measurement of intermolecular forces, *Methods Enzymol.*, 1986, **127**, 400–416.

31 M. Trunec, Osmotic drying of gelcast bodies in liquid desiccant, *J. Eur. Ceram. Soc.*, 2011, **31**, 2519–2524.

32 H. Senff and W. Richtering, Influence of crosslink density on rheological properties of temperature sensitive microgel suspensions, *Colloid Polym. Sci.*, 2000, **278**, 830–840.

33 K. S. Oh, J. S. Oh, H. S. Choi and Y. C. Bae, Effect of crosslinking density on swelling behavior of NIPA gel particles, *Macromolecules*, 1998, **31**, 7328–7335.

34 C. Sayil and O. Okay, Macroporouspoly(N-isopropyl) acrylamide networks: formation conditions, *Polymer*, 2001, **42**, 7639–7652.